DOI: 10.1515/adms-2016-0009

M. Kmieć, B. Karpiński, M. Szkodo

Gdańsk University of Technology, Faculty of Mechanical Engineering, Department of Materials Technology and Welding, 11/12 Narutowicza, 80-233 Gdańsk, Poland
mateusz.kmiec@pg.gda.pl

CAVITATION EROSION OF P110 STEEL IN DIFFERENT DRILLING MUDS

ABSTRACT

The P110 steel specimens were subjected to ultrasonic cavitation erosion in different compositions of drilling muds and surfactant additive. The test procedure was based on ASTM-G-32 standard recommendations. API 5CT- P110 steel is used for pipes in oil and gas industry. The harsh environment and high velocity of flows poses corrosive and erosive threat on materials used there. The composition of drilling fluid influences its rheological properties and thus intensity of cavitation erosion. The erosion curves based on weight loss were measured.

Keywords*: Cavitation erosion, P110 steel, sorbite, surfactant, shear thinning, viscosity, drilling fluid*

INTRODUCTION

Cavitation is a complex and interesting phenomenon that has notable impact on industrial systems and everyday life[1-3]. Every process that involves high velocity flows of liquids, operates within higher temperatures, or involves oscillations of kHz order is prone to cavitation occurrence [4]. The effect of cavitation erosion on P110 steel specimen is shown on Fig. 1 and Fig. 2.

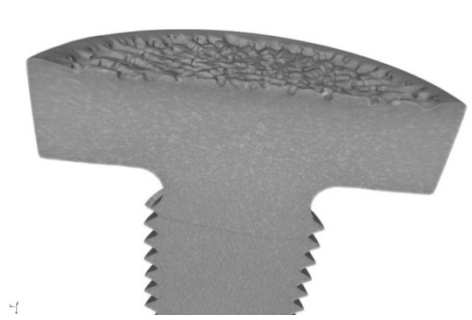

Fig. 1. 3D tomography image of highly eroded test sample

In oil and gas industry, inside the wellbore, high velocity turbulent flows can be observed. In high pressure and high temperature wells (HP/HT) environment is even more hostile. Above all, several kilometer deep well fluids may be rich in highly corrosive CO_2 and H_2S. Materials used in such applications need to withstand cavitation erosion [5] alongside with corrosion especially around their threaded connections [6]. The P110 steel is one of API 5Ct [7] standard pipe steel widely used in oil and gas well construction.

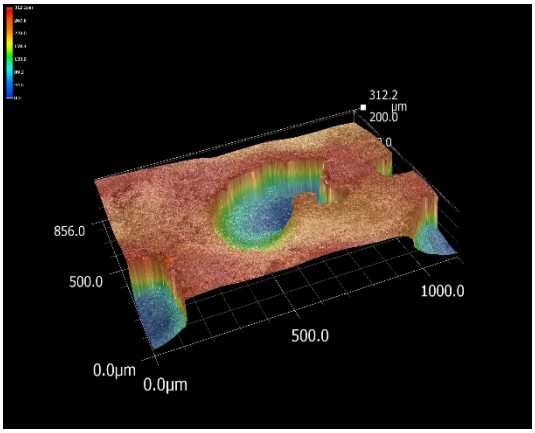

Fig. 2. Microscope 3d image of highly eroded test sample surface

During the drilling process, high volume of (drilling) fluid is circulated into the well. Its function is to compensate for hydrostatic pressure at depth, cool drilling bit, carry out cut rock material or suspend it when the operation stops. It also reduces friction between walls of the hole and drilling equipment. In order to fulfill these requirements, several components are added to modify its rheological and chemical properties.

In order to prevent corrosive degradation of pipes, anti-corrosion agents are added to the drilling fluids. Most corrosion inhibitors used in the industry are organic compounds with N or S functional groups [8]. Those belong to the surfactant agents category that reduces interfacial free energy. The interfacial free energy is an important factor that influences dynamics of cavitation bubble growth and collapse [9].

In downhole conditions, pipe columns fail due to a combination of factors such as: abrasion, erosion, cavitation and strain. This study takes only cavitation erosion under consideration [10].

EXPERIMENTAL

The steel of choice is P110 grade which is defined in American Petroleum Institute 5CT standard that requires it to have at least 758 MPa yield strength (110 PSI). As the standard does not put much restrictions on chemical composition of the steel, the actual one may differ depending on manufacturer. Only the phosphorus and sulphur components are to be under 0.03%. The composition usually stays within values enlisted in Table 1.

Table 1. *P110 steel chemical composition*

Standard	Type	Chemical composition (wt. %)									
		C	Si	Mn	P	S	Cr	Ni	Cu	Mo	V
API 5CT	P110 (300CrMo)	0.26 0.35	0.17 0.37	0.40 0.70	≤0.020	≤0.010	0.80 1.10	≤0.20	≤0.20	0.15 0.25	≤0.08

The total elongation under load is to be under 0.6%. The material needs to be quenched and tempered, but the norm does not define exact temperatures. With the courtesy of Exalo Drilling S.A. we obtained a short piece of 11 3/4 inch casing pipe. Firstly the sample was cut from the pipe to examine microstructure of material. The Fig. 3 shows that the material was quenched and then tempered which resulted in sorbite microstructure with spherical cementite.

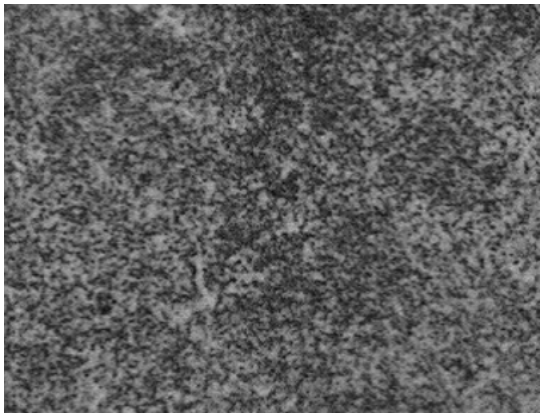

Fig. 3. P110 steel microstructure, magn. 1000x

The measured hardness was 225HV. In order to ensure the best representation of real life parameters, the cavitation test specimens were extracted from the pipe in a manner shown on

Fig. ***4***. The inner surface of the tube is exposed to cavitation erosion and corrosion. The specimens were cut from the tube and then machined into shape, the working surface was then polished down to 600 grit paper without electropolishing.

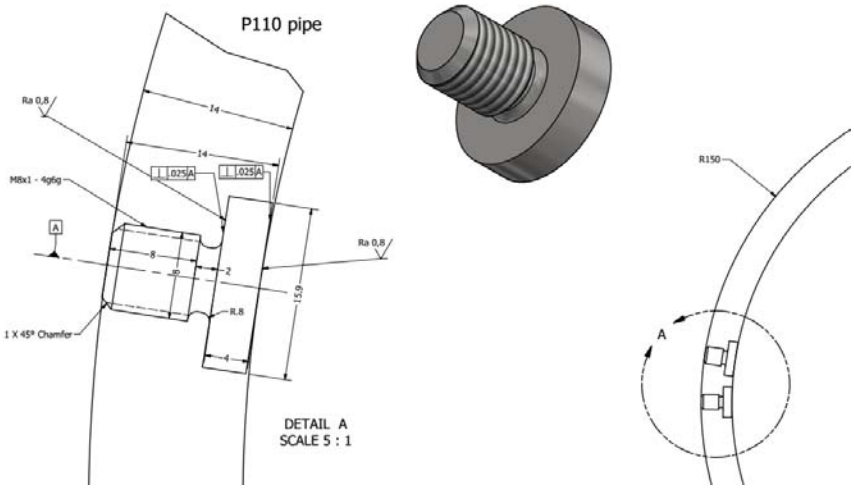

Fig. 4. Test sample technical drawing with extraction position

The cavitation erosion tests were performed using magnetostrictive vibratory apparatus. The tests were conducted in the configuration shown in Fig. 5. Among other methods for achieving cavitation effect, this offers easy control of parameters as well as their repeatability. The test procedure is defined in ASTM G-32[11] standard. The basic part of the apparatus consists of transducer and control unit, which creates longitudinal waves. The waves are amplified by the sonotrode designed as a lambda/2 vibrator. At the end of sonotrode the test specimen is screwed. The specimen has 15.9 mm radius. The specimen vibrates within a cooled vessel filled with liquid, causing cavitation. In the investigation, Hielscher UP400st transducer and control unit were used. It has 400W output power at 90% efficiency, operates at 24 KHz frequency and adjusts it to the sonotrodes parameters in ±500 Hz range. The maximum amplitude (peak to peak) the device can generate using 15.9 tip sonotrode is 0.1mm. During the tests it was set to maintain 50% of maximum amplitude [12] i.e. 50μm. The 25°C temperature was maintained by ultra-thermostat, which circulated cooling agent through cooling bath.

Due to high influence of parameters of cavitating liquid on erosion intensity, the distilled water was used for the reference run as well as a base for variants of drilling fluids. The additives used are as follows: Bentonite OCMA which stabilises the borehole and has, alongside with Antisol 30000 polymer (carboxymethylcellulose)**,** shear-thinning property which guarantees the uplifting of drilled material and higher viscosity [13].

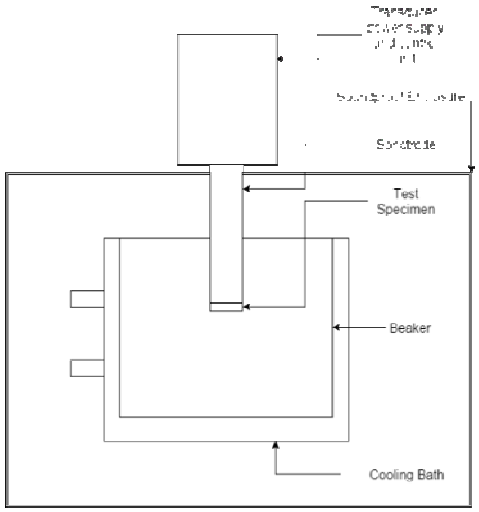

Fig. 5. Test stand schematic

The corrosion inhibitor used in the investigation is SDS – Sodium dodecyl sulfate is a charged surfactant. The surface-active properties come from its amphipathic, lipid like, molecular structure, which contains a polar head group having strong attraction to water, referred to as a hydrophilic head and a non-polar hydrocarbon chain, having little attraction to water, called a hydrophobic tail. With the increased concentration of surfactant, the corrosion inhibition effectiveness increases. Above CMC (critical micelle concentration) the surfactant form multi-layer barrier on interfaces e.g. specimen surface, below it reduces surface tension. The CMC for SDS is 8.3 mMol[14]. Both under and over CMC cases were investigated in this study. The composition of used mediums are shown in Table 2.

Table 2. *Mud compositions*

	MUD I	MUD II	MUD III	SDS 1mM	SDS 10 mM	SDS 1mM +MUD II
Distilled Water [ml]	700	700	700	700	700	700
Bentonite OCMA [g]	7	7	14	0	0	7
Antisol FL 3000 [g]	0.7	1.4	0.7	0	0	1.4
SDS [g]	0	0	0	0.3	3	0.3

The specimens were weighted and then subjected to cavitation erosion on the previously mentioned test stand. After fixed exposure intervals they were detached from the sonotrode, cleaned and precisely weighted again. After pre-tests, the exposure intervals were set to 20,10,10,10,20,20,40,60,90,90 minutes.

RESULTS

Cumulative mass loss curve

The cumulative weight loss after each time period was computed as difference between first measurement and one measured after given time:

$$m_{cl} = m_0 - m_n \quad (1)$$

The cumulative weight loss curves are shown in

Fig. ***6***.

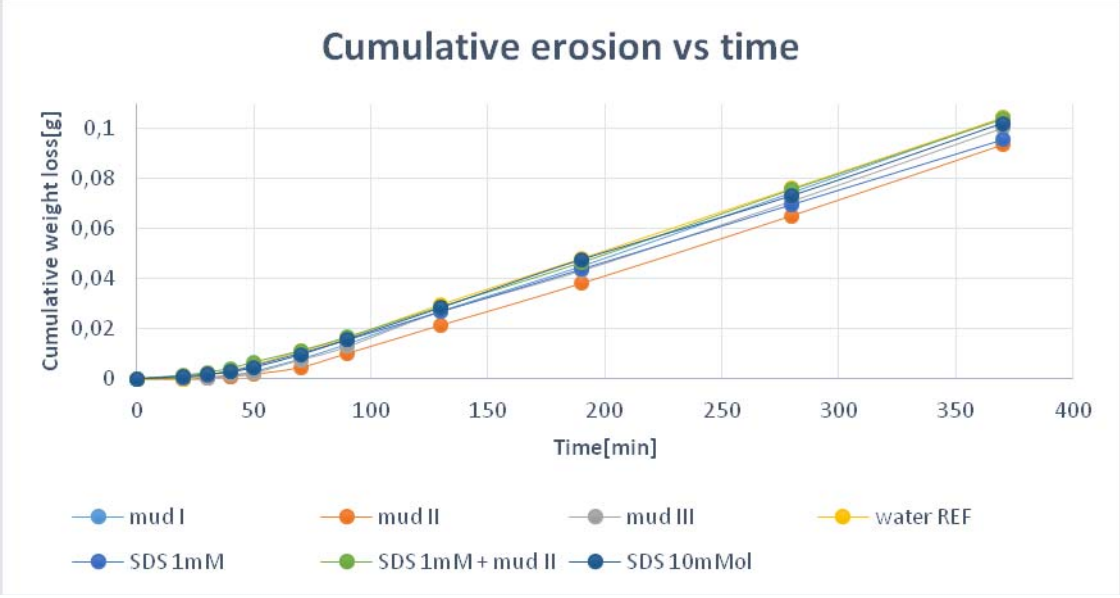

Fig. 6 Cumulative mass loss curves

Erosion Rate Time Curve

As the data is measured in discrete time instances, the derivative can be calculated as backward discrete derivative.

$$\frac{m_n - m_{n-1}}{h} \tag{2}$$

where h - is time interval
The data is shown in

Fig. ***7***

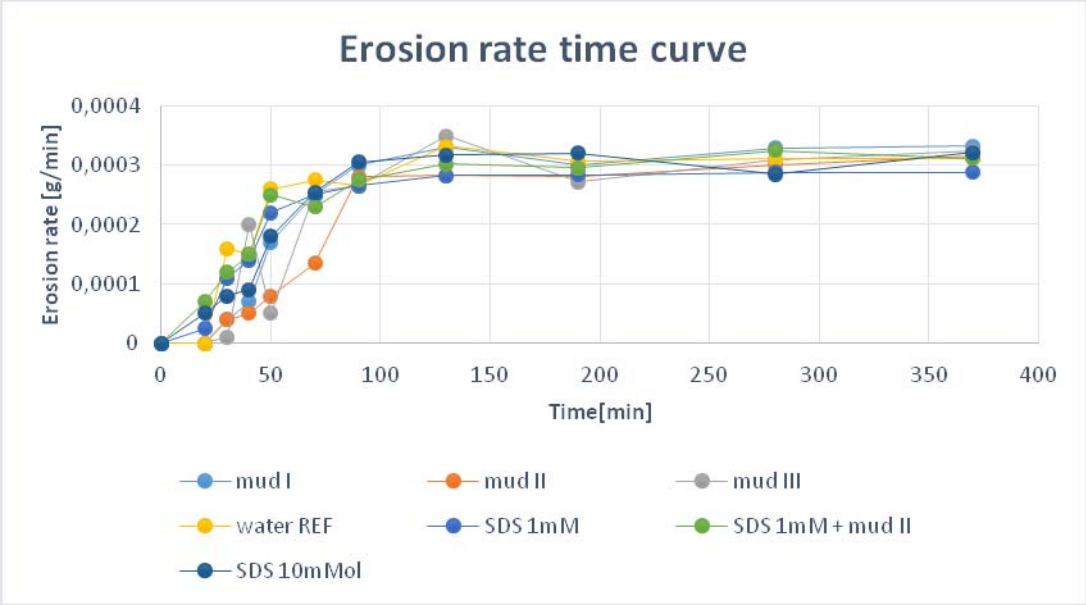

Fig. 7. Cavitation erosion rate time curves

The raw differential was fitted to three parameter Weibull CDF function using nonlinear least mean squares algorithm. The outcome can be observed on Fig. 8.

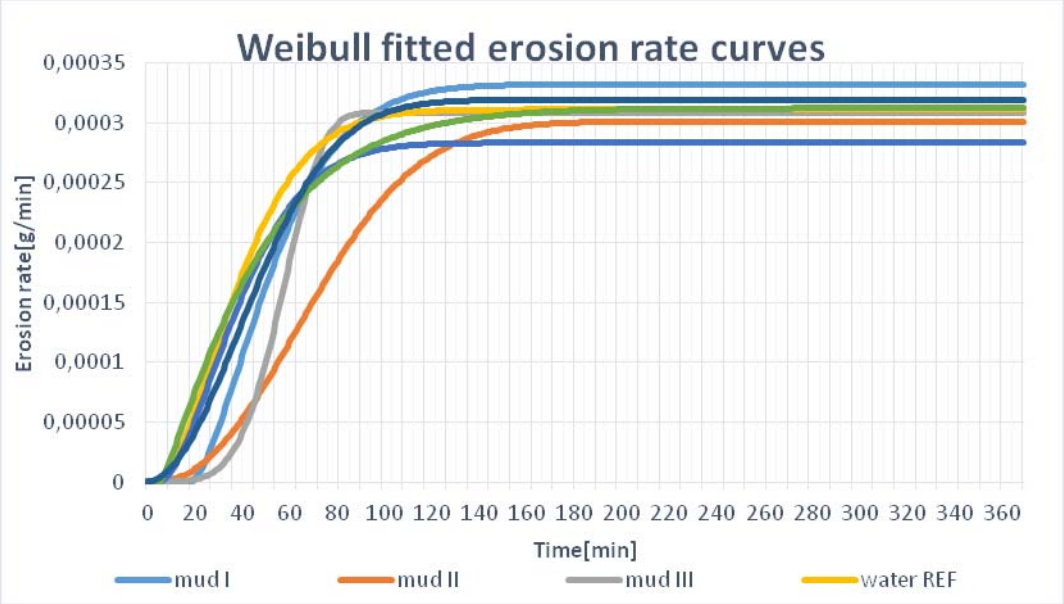

Fig. 8 Weibull fitted erosion rate curves

The mean erosion rate, mean erosion rate in stabilized period (90min) with and without Weibull CDF fitting, and maximum erosion rates are listed in Table 3.

Table 3. *Erosion rates*

	mud I	mud II	mud III	water REF	SDS 1mM	SDS 1mM + mud II	SDS 10mMol
mean erosion rate[µg/min]	1928	1603	1849	2157	1956	2117	2003
Mean erosion after stab. Weibull [µg/min]	3322	3011	3089	3111	2833	3122	3192
mean erosion rate after stabilization [µg/min]	3182	2916	3038	3055	2813	3018	3096
maximum erosion rate [µg/min]	3322	3144	3500	3325	2878	3244	3211

Erosion Threshold Time

By definition it is an exposure time required to reach the mean erosion depth of 1 µm. As the data points are discrete in time, the actual Erosion Threshold Time most probably lay between them. The linear interpolation between data points is chosen as it is the simplest one. $h = 1\mu m$ mean erosion depth, for P110 steel density of d =7.85 g/cm^3 and tip area of a=1.986 cm^2 equals:

$$m = a \cdot h \cdot d = 16 \cdot 10^{-4} g = 1.6mg \quad (3)$$

The time values are listed in Table 4.

Table 4. *Erosion threshold time*

medium	mud I	mud II	mud III	water REF	SDS 1mM	SDS 1mM + mud II	SDS 10mMol
threshold time [min]	43	49	38	30	30	22	28

Nominal Incubation Time

The term by definition is the intercept on the time axis of the straight line extension of the maximum slope portion of the cumulative erosion time curve. Authors find it reasonable to also calculate intersection with mean erosion rate after 90 minutes after which erosion rate stabilizes. The outcome of calculations is shown in Table 5.

Table 5. *Nominal incubation time*

	mud I	mud II	mud III	water REF	SDS 1mM	SDS 1mM + mud II	SDS 10mMol
intersection mean [min]	48	59	47	36	36	38	38
intersection max [min]	55	72	52	40	38	47	52

DISCUSSION

The calculated and plotted data show significant differences in cavitation erosion process of P110 steel. Each plot is discussed in term of visible trends and data validity. The outcomes of factor analysis are grouped into three groups of high, medium and low values and color-marked in the tables. High values are orange, yellow- medium and green denotes low values. The possible processes connecting solution components and factor values are elaborated.

Cumulative mass loss curves

Cumulative mass loss curves shows that mud II and 1mM SDS solution are least erosive environments. The 1mMol SDS solution also has the least steep stabilized slope. Other solutions have comparable data plots with exclusion of mud II which is also significantly less erosive.

Erosion rate time curves

The erosion rate data points are visibly noisy, due to the fact that differentiation of curve amplifies uncertainties. It is common that the curves are not strictly monotonic, which is highly improbable in early stages of degradation.[11] Especially mud III curve has 10e-5 data point on 50 min which may indicate blunder. The values for all curves stabilises around 90 min data point, thus authors considered calculating erosion rate at this segment reasonable. For the sake of readability Weibull CDF fitting was conducted for all curves.

Nominal Incubation Time

The longest incubation time according to maximum slope method was observed with mud II composition, the values for 10mM SDS solution, 1mM SDS + mud II, mud I and III showed values around 50 minutes. Using the 1 mMol SDS solution and water environment has resulted in the shortest incubation periods. The mean stabilized slope method has confirmed the use of mud II to result in the highest value whereas the incubation time around 48 minutes has followed from tests with mud I and mud III. The lowest incubation time was stated for all

SDS solutions. The data shows that bigger concentration of viscosifier Antisol 30000 and Bentonite significantly prolong Nominal Incubation Time. This effect is probably due to reduction of bubble wall velocity and prolongation of the first collapse time of a bubble.[15] According to Gruzdkov and Petrov [16] the energy transferred into the liquid is converted into surface energy of bubbles, work against viscosity and kinetic energy of adjacent layers. Thus the more viscous medium is the bigger fraction of energy is consumed by work against viscosity, and kinetic energy fraction diminishes. As a result the kinetic energy available for surface degradation may be reduced. The mechanism of particle ejection, especially of bentonite particles may also influence the process, however it was investigated for much larger particles[17]. The other factor, present at the interface with degraded surface, may be the bubble-bisection-jet velocity which will be reduced by viscous forces. And thus reducing load on the eroded surface.[15]

Erosion thresholds

The longest erosion threshold was found in mud II composition, mud I and II had slightly lower values, water and SDS water solutions had values around 30min in the middle of scale. The shortest erosion threshold time was noted with mud II and SDS solution. The erosion threshold is a different norm for the incubation time parameter. Thus the bigger values for more viscous liquids may have the same explanation as above.

Mean erosion rates

The lowest mean erosion rate was noted for mud II composition, water and mud II with SDS solution, rest of solutions lay sparsely between, with SDS solutions having slightly higher rates. The values of mean erosion rate after stabilization are lowest in case of SDS 1mM solution and slightly higher for mud II , highest for mud I, the rest of values are concentrated in the middle. Maximum erosion rate was lowest for SDS 1 mMol solution and biggest for mud III. The rest of composition concentrate around 3230[μg/min] and 3320[μg/min], with lower value of mud II outside of clusters. The mean erosion rate shows that mud II and 1mM SDS solutions are visibly least erosive. As for the shear thinning additives, the effect they have on incubation time is prolonged to further stages of cavitation erosion. Nevertheless due to depolymerisation of carboxymethylocelulose the viscosity drops, thus the protective properties of medium diminishes with time.[18] The SDS additive in small concentration below CMC is responsible for inhibition of bubble coalescence and clustering. The bubble population consists of smaller individuals due to the fact that SDS molecules adsorb to bubble surface and act with repulsive force to other bubbles. This process affects the dynamic of single bubble, which, without merging with others, cannot grow to the size when its boundary gets unstable and violently collapse. Furthermore, the effect is more visible in higher frequencies of acoustic load, nevertheless it exists in lower frequencies, influencing cloud and individual bubble dynamics.[19] It is presumed that this explains lower erosion rate of 1mMol SDS solution. On the contrary the concentration above CMC leads to bigger population of nuclei and diminishes the effect of electrostatic repulsion, making the medium (SDS 10mMol) behaviour closer to reference water[20].

SDS solution influence

The data shows that the SDS concentration below CMC despite shorter incubation time ensures lower erosion rates. The SDS concentration above CMC has no significant influence. The lack of visible influence on incubation time may be due to smaller cavitation bubbles, which do not act with sufficient energy to harden the surface.

Shear Thinning additive influence

The shear thinning additives of Antisol polymer and bentonite clearly increased incubation time. The solution with biggest portion of Antisol had longest incubation times and lowest mean erosion rate as well as low mean stabilized erosion rate. Bigger bentonite concentration on the contrary slightly increased erosion rate and decreased incubation time. This may be due to the fact that denser bentonite filled medium caused the device to provide more power, in order to achieve desired amplitude.

Other factors

During the experimental phase several specimens broke between thread and flat section. Prior to this, the amount of power provided by the device doubled. The temperature of sonotrode and specimen rose notably due to friction. After this stage the resonant frequency of sonotrode changed above 500Hz which caused the process to stop and start again with a new specimen. It is advised to use bigger than M8x1 thread for steel specimen. The fluctuations of power may have influenced the outcomes in a straightforward way. Also the friction wear in threaded connection may have accounted for weight loss. Unfortunately it is impossible to easily measure this mass.

CONCLUSIONS

The conducted study shows, that using surfactant additives below CMC concentration as well as additives that highly increases viscosity such as Antisol 30000 are beneficial in case of cavitation erosion. On the contrary Bentonite additive and high surfactant concentration increases cavitation erosion rate. Furthermore in the corrosive environment the longer incubation period achieved with high viscosity polymer may delay corrosion processes, especially with coated casing pipes. On the other hand low SDS concentration may be more beneficial in applications where the most danger comes from cavitation erosion due to its low mean stabilized erosion rate. The amount of gathered data was too low to run correlation tests, which may be more conclusive and produce interesting results. As the further work, the influence of temperature, which is an important factor for cavitation erosion, can be investigated with combination of mud additives. This may be desired with respect to HP/HT challenging wells.

REFERENCES

1. Brennen C.E., Cavitation in medicine. Interface Focus, 5 (2015).
2. Gogate P.R., Kabadi A.M., A review of applications of cavitation in biochemical engineering/biotechnology. Biochemical Engineering Journal, 44 (2009), 60-72.
3. Szkodo M., Estimation of cavitation erosion resistance of materials. Advances in Materials Science, 6 (2006), 43-48.
4. Rosenberg LD. Powerful ultrasonic fields, Nauka Moscow (1968), 18-45.
5. Peng C-h, Liu Z-y, Wei X-z. Failure analysis of a steel tube joint perforated by corrosion in a well-drilling pipe. Engineering Failure Analysis, 25 (2012), 13-28.
6. Smith L. Control of corrosion in oil and gas production tubing. British Corrosion Journal, 34, 4 (1999), 247-53.

7. Institute AP. API 5-CT specification for casing and tubing, 9th edition, 2011.
8. Hernandez S., Linares F.L., Bruzual J., Luzon J.G., Isolation of Potential Corrosion Inhibiting Compounds in Crude Oils. NACE International.
9. Brennen C.E., Cavitation and Bubble Dynamics: Oxford University Press; 1995.
10. Brondel D, Edwars R, Hayman A, Hill D, Mehta S, Semerad T., Corrosion in the Oil industry. Oilfield Review, 6 (1994).
11. ASTM. G32-10 Standard Test Method for Cavitation Erosion Using Vibratory Apparatus, 2010.
12. Ultrasonics H., UP200s/UP400S Instruction manual Ultrasonic processors for Laboratories.
13. Dugan G., The Versatile PAC Polymer. National Driller, 30(1) (2009), 60-72.
14. El-Lateef H.M., Abbasov V.M., Aliyeva L.I., Ismayilov T.A., Some surfactants based on the vegetable oils as CO2 corrosion Inhibitors for mild steel in oilfield formation water. International Journal of Corrosion Scale Inhibition, 4(2) (2015), 162-175.
15. Brujan E.A., Cavitation bubble dynamics in non-Newtonian fluids. Polymer Engineering & Science, 49(3) (2009), 419-431.
16. Gruzdkov A.A, Petrov Y.V., Cavitation breakup of low-and high-viscosity liquids. Technical Physics, 53(3) (2008), 291-295.
17. Arora M., Cavitation Inception on Microparticles: A Self-Propelled Particle Accelerator. Physical Review Letters, 92(17) (2004), 174501.
18. Gronroos A, Pentti P, Hanna K., Ultrasonic degradation of aqueous carboxymethylcellulose: effect of viscosity, molecular mass, and concentration. Ultrasonic Sonochemistry, 15 (2008), 644-652.
19. Mettin R., et al., Imaging of the influence of surfactants on bubble structures. DAGA. Stuttgart 2007, 119-20.
20. Lee J, Kentish S, Matula T.J., Ashokkumar M., Effect of surfactants on inertial cavitation activity in a pulsed acoustic field. The Journal of Physical Chemistry B, 109 (2005), 16860-16865.